IEEE Access
Multidisciplinary | Rapid Review | Open Access Journal

Received December 11, 2019, accepted December 27, 2019, date of publication January 8, 2020, date of current version January 16, 2020.

Digital Object Identifier 10.1109/ACCESS.2020.2965081

Resource Allocation for Hybrid RF/FSO Multi-Channel Multi-Radio Wireless Mesh Networks

YAN ZHAO, WENXIAO SHI, HANYANG SHI, WEI LIU, ZHUO WANG, AND JIADONG ZHANG

College of Communication Engineering, Jilin University, Changchun 130012, China

Corresponding author: Wenxiao Shi (swx@jlu.edu.cn)

This work was supported by the National Natural Science Foundation of China under Grant 61601195.

ABSTRACT The overwhelming data rates in next generation wireless networks impose a burden on the high-capacity network planning. One promising strategy to meet the demand for high-capacity communications is to augment radio frequency (RF) based multi-channel multi-radio (MCMR) wireless mesh network (WMN) by free-space optics (FSO). In this paper, we construct a hybrid RF/FSO MCMR WMN topology and address its resource allocation (RA) problem in terms of interface assignment, channel allocation, routing, FSO link allocation, and topology control. Considering the weather effects on FSO link availability and the fading nature of RF links, the RA problem is formulated as a two-stage optimization problem with the objective of maximizing the network throughput. In our optimization model, we formulate each stage as a mixed integer linear program, and the bottleneck RF links are gradually upgraded by FSO links. To avoid the computational complexity of the second stage optimization, an improved iterated local search algorithm is proposed. Simulation results show that our RA scheme is efficient and the throughput can be enhanced dramatically by proper FSO link augmentation.

INDEX TERMS Resource allocation, multi-channel multi-radio, hybrid RF/FSO networks, wireless mesh networks, mixed integer linear program.

I. INTRODUCTION

Wireless mesh network (WMN) has emerged to address the last-mile Internet connectivity issue [1]. Multi-channel multi-radio (MCMR) functionalities enhance network performance and capacity in WMN [2], [3]. Due to the recent explosive increases of pervasive wireless data applications and mobile devices, MCMR WMNs are still subjected to performance issues such as interference and throughput degradation as network sizes increase [4]. Advanced WMN planning that uses multiple wireless technologies with fewer interference and bandwidth issues is a promising alternative [5]. Free-space optics (FSO) can be leveraged to appropriately augment MCMR WMNs for its low interference, short setup time, and high bandwidth [6], [7]. Despite the advantages, unlike its radio frequency (RF) counterpart, FSO is sensitive to the weather-dependent atmospheric phenomena such as turbulence, scattering, and absorbtion [8]. Therefore, some researchers combine the advantages of RF and FSO technologies and design hybrid RF/FSO links in practice [9]–[11]. Encouraged by their designs, we construct a hybrid RF/FSO MCMR WMN architecture and solve its resource allocation (RA) problem.

For a given MCMR WMN topology, the expected long-term traffic demands are fixed and aggregated in the mesh routers (MRs) which serve as mesh gateways (MGs). In RF-only MCMR WMN, congestion and interference may lead to bottlenecks in some backbone links for the ever-increasing traffic demands of mesh clients (MCs). This issue can be solved by increasing the capacity of the bottleneck links. FSO links can provide high bandwidth and are immune to the interference of RF links. In this paper, we use FSO transceivers to effectively augment MCMR WMN by upgrading a few bottleneck RF links. In what follows, the term upgrade means adding FSO transceivers at a neighboring node pair. In Fig. 1, we illustrate a possible architecture of

The associate editor coordinating the review of this manuscript and approving it for publication was Yanjiao Chen.

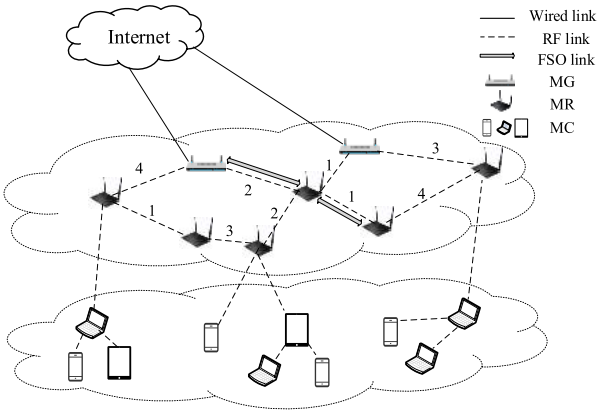

FIGURE 1. Illustration of a hybrid RF/FSO MCMR WMN.

the constructed hybrid RF/FSO MCMR WMN. As shown in Fig. 1, MRs are stationary and form a wireless backbone. Each MR is fitted with more than one network interface card (NIC). The RF NICs operate on different frequency channels. We assume that one of MGs can perform the optimization procedure and RF links are used for signaling. Given the physical topology of the hybrid RF/FSO MCMR WMN, we address the RA problem in terms of interface assignment, channel allocation, topology control, FSO link allocation, and routing.

The RA problem has been studied in several previous works on hybrid RF/FSO networks. The authors of [12] propose an optimal transceiver reconfiguration and formulate the rerouting problem of traffic flow as an integer linear program (ILP) in hybrid RF/FSO WMNs. In [13], the authors introduce a scheme for controlling the topology adaptively to satisfy the specified quality of service (QoS) in hybrid RF/FSO WMNs. The authors of [14] propose a hybrid RF/FSO backhaul strategy to meet the reliability, connectivity, and data rate constraints. In our previous work [15], the joint power control, FSO link allocation, and transmission slot assignment problem is formulated as a mixed integer linear program (MILP) in hybrid RF/FSO WMNs. The authors of [16] propose a joint channel allocation and rate control scheme so as to maximize the throughput of the hybrid RF/FSO vehicular ad-hoc network (VANET). In [17], considering the reliability guarantees of hybrid RF/FSO systems, the authors introduce a joint link selection and power control scheme to minimize power consumption. In the above previous works [12]–[17], the authors only augment single-channel single-radio WMNs with FSO links. However, high interference, intense channel contention, and low network throughput are still the major drawbacks. And the RA problem in the hybrid RF/FSO MCMR WMN is much more challenging and has not been addressed.

Scheduling, routing, and FSO link allocation problems of hybrid RF/FSO WMNs are studied in [6] and [18]. To maximize the network throughput, the authors of [6] augment RF WMN with FSO links and formulate the RF link scheduling and transceiver placement problems as an ILP. In [18], the authors formulate the scheduling, routing, and FSO link allocation as an MILP to enhance the network throughput. There are some differences among [6], [18], and our problem in this paper. First, the complexity is increased in this paper. Their works only focus on solving the scheduling, routing, and FSO link allocation problems for hybrid RF/FSO WMNs. While we address the RA problem for hybrid RF/FSO MCMR WMNs in this paper. Second, to efficiently utilize network resource, we need more sophistication to jointly optimize among the interface assignment, channel allocation, topology control, FSO link allocation, and routing. Third, our model formulation and proposed algorithm are different from [6] and [18].

Some researchers focus on the routing and channel assignment for MCMR WMNs. In [19], the authors use multiple parallel connections to fully utilize the wireless bandwidth and evaluate the performance through real-world experiments. However, the channel assignment and routing of MCMR WMNs are discussed separately, while the global optimization is not investigated for joint channel assignment and routing. To conduct and stimulate the future work on joint channel allocation and routing in MCMR WMNs, the interaction between them is surveyed in [4]. In [20], the authors formulate the joint problem in terms of routing, channel allocation, interface assignment, and logical topology formation as an MILP and use iterated local search (ILS) to solve it. In [21], on-demand channel allocation is proposed and the instantaneous routing demands are met. The authors of [22] introduce an adaptive scheme for coordination and multi-channel assignment in VANET. Nevertheless, congestion and interference create bottlenecks in RF-only MCMR WMNs for the overwhelming date rates in next generation wireless networks.

In this paper, with the goal of alleviating potential congestion and interference, MCMR WMN is upgraded by expanding the bottleneck links with FSO links. Given the physical topology and other constraints of the hybrid RF/FSO MCMR WMN, we address the joint RA problem in terms of routing, topology control, channel allocation, FSO link allocation, and interface assignment. In order to serve more MCs, we devote to maximizing the network throughput for a given number of FSO links. Due to the consideration of deployment cost, we seek to provide the network administrators a theoretical reference to determine the tradeoff between the throughput enhancement and the cost of installing FSO links. The main contributions are summarized as follows:

- We construct a hybrid RF/FSO MCMR WMN topology and tackle its RA problem in terms of interface assignment, channel allocation, routing, FSO link allocation, and topology control. We augment MCMR WMN with FSO links by gradually upgrading the bottleneck RF links with FSO links. To achieve the optimal RA, we conduct a topology configuration, which determines the optimal routing and FSO link placement schemes and meets specified delay QoS, available NIC, and RF channel requirements, all while maximizing the throughput of the hybrid RF/FSO MCMR WMN.

- We jointly formulate the RA problem as a two-stage optimization problem, where each stage is an MILP. In the first stage, we search the bottleneck RF logical links and obtain the initial values for the second stage. In the second stage, we gradually upgrade the bottleneck links with FSO links and solve the RA problem. Our model formulation incorporates the fading nature of RF links and the availability of FSO links under various weather conditions, which is more realistic.
- A high-efficiency and low-complexity algorithm is proposed to solve the two-stage optimization problem, and various simulation results show that our model formulation determines reasonable RA. We obtain the exact initial values by solving the first stage optimization with the efficient commercial software Gurobi, which is appropriate to the alterations of traffic demands. To reduce the computational complexity of the second stage optimization, an improved iterated local search algorithm (IILSA) is proposed. We use ILS and branch-and-cut algorithms to provide baselines for comparisons and show the efficiency of our IILSA. The results of this paper provide insights for the network planning of hybrid RF/FSO MCMR WMNs.

The paper is structured as follows. The underlying network model is described in Section II. In Section III, we formulate RA in terms of routing, topology control, channel allocation, FSO link allocation, and interface assignment as a two-stage optimization. We propose a low-complexity IILSA to solve our two-stage optimization in Section IV. In Section V, the two-stage optimization is addressed via IILSA and Gurobi, and numerical simulation results are provided. Finally, conclusions are drawn and future trajectory of our research effort is presented in Section VI.

II. NETWORK MODEL

In this section, we present the underlying network models for hybrid RF/FSO MCMR WMNs, the RF link availability, and the FSO link availability under various weather conditions.

A. PHYSICAL MODEL AND RF LINK AVAILABILITY

We model the overall network as a directed graph $\mathbb{G} = (N, L)$, where N denotes the vertex (i.e., the node) set and L represents the feasible link set of the hybrid RF/FSO MCMR WMN. Let $l_{mn} \in L$ denotes the directed link from nodes $m \in N$ to $n \in N$, and the connectivity is assumed to be symmetric, that is, link $l_{mn} \in L$ if and only if $l_{nm} \in L$. We assume that each node can be fitted with omnidirectional RF transceivers and directional FSO transceivers. A link is feasible, i.e., $l_{mn}^{RF} \in L$, when the signal-to-noise ratio (SNR) meets [23]:

$$SNR_{mn} = \frac{G_{mn}P_m}{N_0} \geq \phi, \tag{1}$$

where G_{mn} is the channel gain between nodes m and n, P_m is the transmission power of node m, N_0 is the noise power spectral density of the receiver, and ϕ identifies the SNR threshold. We assume that N_0 is fixed and the same for all nodes. $G_{mn} = (d_{mn}/d_0)^{-\eta}$, where d_{mn} is the distance between nodes m and n, η represents the path loss exponent, and d_0 is the close-in reference distance.

When there is interference, links can transmit successfully and simultaneously if their signal-to-interference-plus-noise ratios (SINRs) meet [24]:

$$SINR_{mn} = \frac{G_{mn}P_m}{N_0 + \sum_{k:k\neq m} G_{kn}P_k} \geq \phi. \tag{2}$$

The availability of the link l_{mn}^{RF} is denoted as π_{mn}^{RF}, in Nakagami fading, it can be derived as [25]:

$$\pi_{mn}^{RF} = e^{-\beta_0 z} \sum_{u=0}^{U_m-1} (\beta_0 z)^u \sum_{g=0}^{u} \frac{z^{-g} H_g(\Psi)}{(u-g)!}, \tag{3}$$

where

$$\Psi_k = (\beta_0 \frac{\Omega_k}{U_k} + 1)^{-1}, \quad k \in N\ (k \neq m, n), \tag{4}$$

$$H_g(\Psi) = \sum_{\substack{v_k \geq 0 \\ \sum_{k=0}^{N-2} v_k = g}} \prod_{k=1}^{N-2} B_{v_k}(\Psi_k), \tag{5}$$

$$B_v(\Psi_k) = \begin{cases} 1 - \chi_k(1 - \Psi_k^{U_k}), & v = 0, \\ \frac{\chi_k \Delta(v+U_k)}{v!\Delta(U_k)} (\frac{\Omega_k}{U_k})^v \Psi_k^{U_k+v}, & v > 0, \end{cases} \tag{6}$$

where U_k is the Nakagami parameter of node k, χ_k is the activity probability of node k, $z = \Delta^{-1}$, $\Delta = (d_0)^\eta P_m/N_0$ is SNR_{mn} when d_{mn} is the unit distance, and $v \in \{0, \ldots, U_m - 1\}$. $\beta_0 = \phi U_m/\Omega_m$, where Ω_m is the normalized received power due to the transmitter of node m and derived as [25]:

$$\Omega_k = \begin{cases} 10^{\zeta_k/10} d_{kn}^{-\eta}, & k = m, \\ \frac{aP_k}{WP_m} 10^{\zeta_k/10} d_{kn}^{-\eta}, & k \in N,\ k \neq m, n, \end{cases} \tag{7}$$

where a is the chip factor, W is the spreading factor or processing gain, and ζ_k is the shadowing factor of node k.

B. FSO LINK AVAILABILITY

In this paper, we assume that the optical wave propagates through the log-normal turbulence channel with additive white Gaussian noise (AWGN) under various weather conditions. The FSO channel uses intensity modulation/direct detection (IM/DD) with on-off keying (OOK) [26]. We model the received electrical signal as $y = Rhx + n_0$, where R is the photodetector responsivity, x is the modulated OOK symbol that takes values 0 or $2P_1$ equally likely, P_1 is the average optical transmission power, h is the irradiance of FSO channel, and n_0 is zero-mean AWGN with variance $\sigma_{n_0}^2$ [27]. We assume that there is an active tracking mechanism to eliminate the misalignment fading (i.e., pointing error) effects [28]. Accordingly, h can be expressed as $h = h_a h_p$, where h_p is the turbulence-induced fading and h_a is the path loss [29]. The path loss can be derived as $h_a = \left[erf\left(\sqrt{A}\Big/(\theta d_{mn})\right)\right]^2 e^{-\alpha d_{mn}}$, where $erf(\cdot)$ is the

error function, θ denotes the beam divergence angle, α is the weather-dependent attenuation factor, and $A = \pi r^2/4$ represents the receiver aperture area with diameter r [30].

Under foggy or clear weather conditions, the attenuation per unit length is derived by Kim's model as $\alpha = (3.91/V)(\lambda_1/\lambda_0)^{-q}$, where λ_1 is the optical wavelength, V is the visibility range, q is a constant determined by the scattering particle distribution, and $\lambda_0 = 550$ nm denotes the reference wavelength [31]. For rainy weather, the attenuation per unit length is derived as $\alpha = 1.076\Gamma^{0.67}$ according to the rainfall rate Γ [32].

We define the instantaneous electrical SNR of the FSO link as $\gamma = \gamma_1 h_p^2$, where $\gamma_1 = R^2 h_a^2 P_1^2/\sigma_{n_0}^2$ represents the average SNR. We define the outage probability as the probability that SNR drops below a threshold γ_{th} and it can be derived as [31]:

$$P_{out,mn}^{FSO}(d_{mn}) = Q\left(\frac{\ln\left(h_a(d_{mn})P_1/P_{th1}\right) - \sigma_I^2(d_{mn})/2}{\sigma_I(d_{mn})}\right), \quad (8)$$

where $Q(x) = \frac{1}{\sqrt{2\pi}}\int_x^\infty e^{-t^2/2}dt$ represents the Gaussian Q-function and $P_{th1} \triangleq \sqrt{\gamma_{th}\sigma_{n_0}^2/R^2}$ denotes the transmission power threshold [31]. In (8), σ_I^2 is the scintillation index for the aperture-averaged spherical wave and defined as [33]:

$$\sigma_I^2 = \exp\left[\frac{0.49\sigma_1^2}{\left(1+0.18r_1^2+0.56\sigma_1^{12/5}\right)^{7/6}} + \frac{0.51\sigma_1^2\left(1+0.69\sigma_1^{12/5}\right)^{-5/6}}{1+0.90r_1^2+0.62r_1^2\sigma_1^{12/5}}\right] - 1, \quad (9)$$

where σ_1^2 is the Rytov variance, $k_1 = 2\pi/\lambda_1$ is the optical wave number, and $r_1 = \sqrt{k_1 r^2/4d_{mn}}$. $\sigma_1^2 = 0.492C_n^2 k_1^{7/6} d_{mn}^{11/6}$, where C_n^2 represents the atmospheric refractive index structure constant. We assume that C_n^2 takes values according to the atmospheric turbulence conditions (e.g., clear air, moderate fog, moderate rain, etc.). We can note that the outage probability is distance-dependent. We define the FSO link availability π_{mn}^{FSO} as the probability that an FSO link transmits successfully, thus it can be obtained as:

$$\pi_{mn}^{FSO} = \Pr(\gamma \geq \gamma_{th}), \quad (10)$$

that is, $\pi_{mn}^{FSO} = 1 - P_{out,mn}^{FSO}$.

III. RESOURCE ALLOCATION PROBLEM

In this section, with a goal of maximizing the network throughput, we jointly formulate the RA problem in terms of routing, topology control, channel allocation, FSO link allocation, and interface assignment as a two-stage optimization problem, while guaranteeing fairness to all traffic demands and satisfying the delay specification. Because of the high cost of FSO components compared to RF components [34], the results of our model formulation can be used for network administrators to determine the tradeoff between the throughput enhancement and the cost of installing FSO links.

A. PROBLEM DEFINITION

Generally, a limited number of RF NICs is available in MCMR WMNs, which implies that an RF NIC may be required to share by some logical links in an MR to receive and transmit data packets. In other words, the logical links in an MR need to operate on the identical RF channel. The logical links in an MR cannot be active simultaneously when they share one RF NIC, which reduces their actual capacity significantly. To avoid the congestion in some links leading to bottlenecks, higher capacity of backbone links are needed as the traffic demands of MCs increase. We can enhance the backbone link capacity by augmenting the bottleneck RF links with FSO links. In practice, an existing RF network can be upgraded by installing FSO links, for FSO and RF links do not interfere with each other. Given the physical topology of the RF network and expected long-term traffic demands, we study the throughput optimization achieved by installing FSO links in MCMR WMNs, while guaranteeing fairness to the given traffic demands and satisfying the end-to-end delay requirement. Furthermore, we address the RA problem in terms of five important issues in the hybrid RF/FSO MCMR WMNs: interface assignment, channel allocation, routing, FSO link allocation, and topology control. Our objective is to maximize the throughput of the hybrid RF/FSO MCMR WMNs by proper RA. The objectives and constraints are formulated as a two-stage optimization:

Stage 1: The optimized minimum normalized flow over all source-destination pairs and the bottleneck RF logical links across the network are found. In addition, the sets of logical links that can satisfy the interface and channel constraints are obtained.

Stage 2: Based on the solutions obtained from the first stage, the bottleneck RF links are gradually upgraded with FSO links. In the constructed hybrid RF/FSO MCMR WMNs, with the objective of improving the minimum normalized flow over all source-destination pairs, the RA problem in terms of routing, topology control, channel allocation, FSO link allocation, and interface assignment is solved.

The tuning of RF and FSO transceivers can be done in less than 1 ns, that is, the switching delay caused by tuning is negligible [12], so the switching procedure is not detailed in this paper. We consider the data can be buffered if the channel fading happens and transmitted once the link recovers. The details of such buffer and retransmission schemes are outside the scope of this paper. We assume that the expected long-term traffic demands of the network are seldom changed. In other words, the traffic demands are changeless within a time period, which is long enough to obtain the optimal solutions of our optimization problem. Network operates on these optimized solutions until the changes of traffic demands.

B. PROBLEM FORMULATION

Based on the above definition, we detail the two-stage optimization which is used to solve our RA problem in this subsection.

1) FLOW CONSERVATION CONSTRAINTS

In a network, flows cannot be terminated or generated on any nodes except for destination nodes and source nodes, we require $\forall m, n, v \in N$ and $\forall \omega \in S_D$:

$$\sum_{l_{vn}\in L}\sum_{i=1}^{C}\lambda_{vn,i}^{\omega}-\sum_{l_{mv}\in L}\sum_{i=1}^{C}\lambda_{mv,i}^{\omega}=\begin{cases}f_{\omega}, & v=s,\\ -f_{\omega}, & v=d,\\ 0, & \text{otherwise},\end{cases} \tag{11}$$

where ω is the source-destination pair, s and d denote the source and destination of ω respectively, C denotes the number of available RF channels, f_ω denotes the actual traffic flow of ω, S_D is the set of traffic demand connections, and finally, $\lambda_{vn,i}^{\omega}$ denotes the portion of traffic from connection ω which is carried by the feasible link l_{vn} over the i^{th} RF channel.

For the second stage where the bottleneck RF links are upgraded by installing FSO links, the flow conservation constraint can be defined as $\forall m, n, v \in N$ and $\forall \omega \in S_D$:

$$\sum_{l_{vn}\in L}\sum_{i=1}^{C}\lambda_{vn,i}^{\omega}+\sum_{l_{vn}\in L}\lambda_{vn,FSO}^{\omega}-\sum_{l_{mv}\in L}\sum_{i=1}^{C}\lambda_{mv,i}^{\omega}-\sum_{l_{mv}\in L}\lambda_{mv,FSO}^{\omega}=\begin{cases}f_{\omega}, & v=s,\\ -f_{\omega}, & v=d,\\ 0, & \text{otherwise},\end{cases} \tag{12}$$

where $\lambda_{vn,FSO}^{\omega}$ is the portion of traffic from connection ω carried by the logical link l_{vn}^{FSO}.

2) ROUTING CONSTRAINTS

In order to avoid the disorder of the data packets belong to the identical flow, which is caused by forwarding the packets on parallel logical links between the neighboring nodes, we require $\forall m, n \in N, l_{mn} \in L, \forall \omega \in S_D$:

$$\sum_{i=1}^{C}Y_{mn,i}^{\omega}\le 1, \tag{13}$$

where $Y_{mn,i}^{\omega}$ is an indicator variable of routing, and $Y_{mn,i}^{\omega}=1$ if $\lambda_{mn,i}^{\omega}>0$, otherwise $Y_{mn,i}^{\omega}=0$. If the bottleneck RF links are upgraded with FSO links, to avoid the above-mentioned disorder and the incompatibility of RF and FSO link data rates, we require that $\forall m, n \in N, l_{mn} \in L, \forall \omega \in S_D$:

$$\sum_{i=1}^{C}Y_{mn,i}^{\omega}+Y_{mn,FSO}^{\omega}\le 1, \tag{14}$$

where $Y_{mn,FSO}^{\omega}$ is another indicator variable of routing, and $Y_{mn,FSO}^{\omega}=1$ if $\lambda_{mn,FSO}^{\omega}>0$, otherwise $Y_{mn,FSO}^{\omega}=0$.

For a fraction of time, only the RF logical links which do not interfere with each other can be active. To ensure that the logical link cannot transmit successfully and simultaneously with the potential interfering links, we require that $\forall m, n \in N, l_{mn} \in L, \forall i = 1, \ldots, C$:

$$\frac{c_{mn}^{i}}{c^{RF}\pi_{mn}^{RF}}+\sum_{\substack{j,h\in N,\\ l_{jh}\in E_{mn}}}\frac{c_{jh}^{i}}{c^{RF}\pi_{jh}^{RF}}\le 1, \tag{15}$$

where $c_{mn}^{i}\ge 0$ is the actual capacity of the logical link l_{mn}^{RF}, c^{RF} is the nominal link rate of RF link, E_{mn} is the set of links which interfere with l_{mn}^{RF} potentially, and $c_{mn}^{i}/(c^{RF}\pi_{mn}^{RF})$ is the fraction of time that the logical link l_{mn}^{RF} is active.

3) FSO LINK ALLOCATION CONSTRAINTS

In order to define the FSO links which are used to gradually upgrade the bottleneck RF links, we require:

$$D_{mn}^{FSO}=\begin{cases}1, & \min\limits_{\substack{m,n\in N, l_{mn}\in L,\\ i\in\{1,\ldots,C\},\\ x_{mn}^{i}=1}}\left(c_{mn}^{i}-\sum\limits_{\omega}\lambda_{mn,i}^{\omega}\right),\\ 0, & \text{otherwise},\end{cases} \tag{16}$$

where D_{mn}^{FSO} and x_{mn}^{i} are the indicator variables of the FSO link and channel allocation, respectively. $D_{mn}^{FSO}=1$ if there is an FSO link from m to n, otherwise $D_{mn}^{FSO}=0$. $x_{mn}^{i}=1$ if node m communicates with n using the i^{th} RF channel in the logical topology, otherwise $x_{mn}^{i}=0$. Note that $D_{mn}^{FSO}=1$ corresponds to the bottleneck RF logical link, that is, the most congested RF logical link from node m to node n is upgraded by installing FSO logical link from m to n.

The commercial FSO units support full-duplex communications [35], thus we have $\forall m, n \in N, l_{mn} \in L$:

$$D_{nm}^{FSO}=D_{mn}^{FSO}. \tag{17}$$

To limit the total number of FSO upgrades, we require that $\forall m, n \in N, l_{mn} \in L$:

$$\frac{1}{2}\sum_{\substack{m,n\in N,\\ l_{mn}\in L}}D_{mn}^{FSO}=M, \tag{18}$$

where M is the total number of FSO upgrades to be installed.

4) CHANNEL ALLOCATION, INTERFACE ASSIGNMENT, AND LOGICAL TOPOLOGY CONSTRAINTS

In the logical topology, each neighboring node pair should be assigned the identical frequency channel to communicate with each other, we require $\forall m, n \in N, l_{mn} \in L, \forall i = 1, \ldots, C$:

$$x_{mn}^{i}=x_{nm}^{i}. \tag{19}$$

The total number of RF channels used to establish logical topology is less than or equal to the total number of RF NICs, for each RF NIC operates on the distinct channel. To ensure this, we require that $\forall m \in N$:

$$\sum_{i=1}^{C}y_{m}^{i}\le I, \tag{20}$$

where I is the number of available RF NICs and y_{m}^{i} is an indicator variable of node channel allocation. For $\forall i = 1, \ldots, C$ and $\forall m \in N$, $y_{m}^{i}=1$ if $n \in N$, $l_{mn} \in L$, and $x_{mn}^{i}=1$. According to the definitions of the indicator variables, we have that $\forall m, n \in N, l_{mn} \in L, \forall i = 1, \ldots, C$:

$$x_{mn}^{i}\le y_{m}^{i}, \tag{21}$$

$$y_{m}^{i}\le\sum_{n\in N, l_{mn}\in L}x_{mn}^{i}. \tag{22}$$

5) CAPACITY CONSTRAINTS

For the actual capacity and the nominal link rate of an RF logical link, we have $\forall m, n \in N$, $l_{mn} \in L, \forall i = 1, \ldots, C$:

$$c_{mn}^{i} \leq x_{mn}^{i} c^{RF} \pi_{mn}^{RF}. \tag{23}$$

In order to ensure that the aggregated traffic of l_{mn}^{RF} is less than or equal to the actual capacity, we require $\forall m, n \in N$, $l_{mn} \in L, \forall i = 1, \ldots, C$:

$$\sum_{\omega \in S_D} \lambda_{mn,i}^{\omega} \leq c_{mn}^{i}. \tag{24}$$

In the second stage optimization, for the condition that the bottleneck RF logical links are upgraded with FSO links, to ensure that the aggregated traffic passing through the FSO logical link does not exceed the available link capacity, we require that $\forall m, n \in N, l_{mn} \in L$:

$$\sum_{\omega \in S_D} \lambda_{mn,FSO}^{\omega} \leq D_{mn}^{FSO} c^{FSO} \pi_{mn}^{FSO}, \tag{25}$$

where c^{FSO} is the FSO link capacity.

6) DELAY QoS CONSTRAINTS

In order to ensure that the hop count along the assigned route satisfies the delay requirement, we have $\forall \omega \in S_D$:

$$\sum_{m,n \in N, l_{mn} \in L} \sum_{i=1}^{C} Y_{mn,i}^{\omega} \leq \xi h_G^{\omega}, \tag{26}$$

where h_G^{ω} is the hop count of the min-hop path for the connection ω in the physical topology graph G, and $\xi \geq 1$ denotes a tunable parameter. We note that ξ sets an upper bound on routing stretch factor $\sum_{\substack{m,n \in N, \\ l_{mn} \in L}} \sum_{i=1}^{C} Y_{mn,i}^{\omega} / h_G^{\omega}$. For the second stage that the FSO links are used as the link upgrades, we require that $\forall \omega \in S_D$:

$$\sum_{\substack{m,n \in N, \\ l_{mn} \in L}} \sum_{i=1}^{C} Y_{mn,i}^{\omega} + \sum_{\substack{m,n \in N, \\ l_{mn} \in L}} Y_{mn,FSO}^{\omega} \leq \xi h_G^{\omega}. \tag{27}$$

7) OBJECTIVE FUNCTION AND FAIRNESS CONSTRAINT

We take advantage of the weighted fairness concept to guarantee the network fairness, we require $\forall \omega \in S_D$:

$$d_{\omega} \times F \leq f_{\omega}, \tag{28}$$

where d_{ω} is the given traffic demand of ω, and F is the minimum normalized flow over all ω. The objective of maximizing the network throughput while guaranteeing fairness to all traffic demands can then be achieved by maximizing F.

C. TWO-STAGE OPTIMIZATION

We now summarize our two-stage optimization. Please refer to Table 1 for notations. Given the RF physical topology $G = (N, L)$ and the parameters c^{RF}, c^{FSO}, E_{mn}, ξ, h_G^{ω}, M, ω, d_{ω}, C, I, the two-stage optimization is formulated as an MILP in each stage as follows:

TABLE 1. Symbol description.

Symbol	Description
F	The minimum normalized flow over all connections ω
$\lambda_{mn,i}^{\omega}$	The portion of traffic from connection ω carried by the feasible link l_{mn}^{RF} over the i^{th} RF channel
$\lambda_{mn,FSO}^{\omega}$	The portion of traffic from connection ω carried by the logical link l_{mn}^{FSO}
c_{mn}^{i}	The actual capacity of the logical link l_{mn}^{RF}, and $c_{mn}^{i} \geq 0$
c^{RF}	The nominal link rate of an RF logical link
c^{FSO}	Link capacity of an FSO logical link
E_{mn}	The set of links which interfere with each other potentially
ξ	The tunable parameter to set an upper bound on the routing stretch factor, and $\xi \geq 1$
h_G^{ω}	The hop count for the minimum hop path between the connection ω in the physical topology graph G
M	The total number of the FSO links which are to be installed
x_{mn}^{i}	$x_{mn}^{i} = 1$ if node m communicates with node n over the i^{th} RF channel in the logical topology; otherwise $x_{mn}^{i} = 0$
y_m^i	$y_m^i = 1$ if $x_{mn}^{i} = 1$, where $\exists n \in N$ and $l_{mn} \in L$
D_{mn}^{FSO}	$D_{mn}^{FSO} = 1$ if there is an FSO link upgrade from m to n; otherwise $D_{mn}^{FSO} = 0$
$Y_{mn,i}^{\omega}$	$Y_{mn,i}^{\omega} = 1$ if $\lambda_{mn,i}^{\omega} > 0$; $Y_{mn,i}^{\omega} = 0$ if $\lambda_{mn,i}^{\omega} = 0$
$Y_{mn,FSO}^{\omega}$	$Y_{mn,FSO}^{\omega} = 1$ if $\lambda_{mn,FSO}^{\omega} > 0$; $Y_{mn,FSO}^{\omega} = 0$ if $\lambda_{mn,FSO}^{\omega} = 0$
s, d, ω, S_D	Source, destination, source-destination pair, and set of traffic demand connections
d_{ω}, f_{ω}	The given traffic demand and actual traffic flow of $\omega \in S_D$
C, I	Available RF channels and NICs

- The first stage:

$$\underset{\lambda, x, y, Y, c, f, F}{\textbf{maximize}} \quad F$$

subject to

$$C1: \sum_{l_{vn} \in L} \sum_{i=1}^{C} \lambda_{vn,i}^{\omega} - \sum_{l_{mv} \in L} \sum_{i=1}^{C} \lambda_{mv,i}^{\omega} = \begin{cases} f_{\omega}, & v = s, \\ -f_{\omega}, & v = d, \\ 0, & \text{otherwise}, \end{cases} \quad \forall m, n, v \in N, \ \forall \omega \in S_D,$$

$$C2: \sum_{i=1}^{C} Y_{mn,i}^{\omega} \leq 1, \quad \forall m, n \in N, \ l_{mn} \in L, \ \forall \omega \in S_D,$$

$$C3: \sum_{m,n \in N, l_{mn} \in L} \sum_{i=1}^{C} Y_{mn,i}^{\omega} \leq \xi h_G^{\omega}, \quad \forall \omega \in S_D,$$

$$C4: \sum_{i=1}^{C} y_m^i \leq I, \quad \forall m \in N,$$

$$C5: x_{mn}^{i} = x_{nm}^{i}, \quad \forall m, n \in N, \ l_{mn} \in L, \ \forall i = 1, \ldots, C,$$

$$C6: x_{mn}^{i} \leq y_m^i, \quad \forall m, n \in N, \ l_{mn} \in L, \ \forall i = 1, \ldots, C,$$

$$C7: y_m^i \leq \sum_{n \in N, \ l_{mn} \in L} x_{mn}^{i}, \quad \begin{matrix} \forall m, n \in N, \ l_{mn} \in L, \\ \forall i = 1, \ldots, C, \end{matrix}$$

$$C8: c_{mn}^{i} \leq x_{mn}^{i} c^{RF} \pi_{mn}^{RF}, \quad \begin{matrix} \forall m, n \in N, \ l_{mn} \in L, \\ \forall i = 1, \ldots, C, \end{matrix}$$

$$C9: \frac{c_{mn}^{i}}{c^{RF} \pi_{mn}^{RF}} + \sum_{\substack{j,h \in N, \\ l_{jh} \in E_{mn}}} \frac{c_{jh}^{i}}{c^{RF} \pi_{jh}^{RF}} \leq 1, \quad \begin{matrix} \forall m, n \in N, \ l_{mn} \in L, \\ \forall i = 1, \ldots, C, \end{matrix}$$

$$C10: \sum_{\omega \in S_D} \lambda_{mn,i}^{\omega} \le c_{mn}^{i}, \quad \forall m,n \in N, l_{mn} \in L, \forall i = 1,\ldots,C,$$
$$C11: d_{\omega} \times F \le f_{\omega}, \quad \forall \omega \in S_D. \tag{29}$$

- The second stage:

With the solutions obtained by solving the above optimization problem (29), the bottleneck RF links are obtained, then we gradually upgrade the bottleneck RF links with FSO links and formulate the RA problem as (30):

$$\underset{\lambda,x,y,Y,c,D,f,F}{\textbf{maximize}} \quad F$$
$$\textbf{subject to}$$
$$C4 \sim C11$$
$$C12: D_{mn}^{FSO} = \begin{cases} 1, & \min\limits_{\substack{m,n\in N, l_{mn}\in L,\\ i\in\{1,\ldots,C\},\\ x_{mn}^{i}=1}} \left(c_{mn}^{i} - \sum\limits_{\omega} \lambda_{mn,i}^{\omega}\right), \\ 0, & \text{otherwise}, \end{cases}$$
$$C13: D_{nm}^{FSO} = D_{mn}^{FSO}, \quad \forall m,n \in N, l_{mn} \in L,$$
$$C14: \sum_{l_{vn}\in L}\sum_{i=1}^{C} \lambda_{vn,i}^{\omega} + \sum_{l_{vn}\in L} \lambda_{vn,FSO}^{\omega} - \sum_{l_{mv}\in L}\sum_{i=1}^{C} \lambda_{mv,i}^{\omega} - \sum_{l_{mv}\in L} \lambda_{mv,FSO}^{\omega} = \begin{cases} f_{\omega}, & v = s, \\ -f_{\omega}, & v = d, \\ 0, & \text{otherwise}, \end{cases} \quad \forall m,n,v \in N, \forall \omega \in S_D$$
$$C15: \sum_{i=1}^{C} Y_{mn,i}^{\omega} + Y_{mn,FSO}^{\omega} \le 1, \quad \forall m,n \in N,\ l_{mn} \in L, \forall \omega \in S_D,$$
$$C16: \sum_{\substack{m,n\in N,\\ l_{mn}\in L}}\sum_{i=1}^{C} Y_{mn,i}^{\omega} + \sum_{\substack{m,n\in N,\\ l_{mn}\in L}} Y_{mn,FSO}^{\omega} \le \xi h_{G}^{\omega}, \quad \forall \omega \in S_D,$$
$$C17: \frac{1}{2} \sum_{\substack{m,n\in N,\\ l_{mn}\in L}} D_{mn}^{FSO} = M,$$
$$C18: \sum_{\omega\in S_D} \lambda_{mn,FSO}^{\omega} \le D_{mn}^{FSO} c^{FSO} \pi_{mn}^{FSO}, \quad \forall m,n \in N,\ l_{mn} \in L. \tag{30}$$

Let the cardinalities of sets N, L, and ω are represented by $|N|$, $|L|$, and $|\omega|$ respectively. The first stage has $(|L|C+1)(|\omega|+1)$ real variables, $|L|(|\omega|+1)C + |N|C$ integer variables, $|L|(|\omega|+4C)+2|\omega|+|N|(C+1)$ inequality constraints, and $|N||\omega| + 0.5|L|C$ equality constraints. The second stage has $|L|(C|\omega| + |\omega| + C) + |\omega| + 1$ real variables, $|L|(C + C|\omega| + |\omega| + 1) + |N|C$ integer variables, $|L|(4C + |\omega| + 1) + |N|C + 2|\omega|$ inequality constraints, and $|L|(0.5C + 1.5) + |N||\omega| + 1$ equality constraints.

The values of decision variables $F, f, c, x, y, Y, \lambda, D$ provide the solution to the problem of how one can attain the maximum network throughput by proper RA, that is, channel allocation, interface assignment, topology control, routing, and FSO link allocation. The two-stage optimization problem is non-convex. The complexity of MILP is dependent on the numbers of constraints and variables and not polynomial in the numbers. In the following, to avoid the complexity of our model formulation, we propose an efficient algorithm to solve it and obtain our RA solutions.

IV. IMPROVED ITERATED LOCAL SEARCH ALGORITHM

There are several effective commercial optimization solvers for MILP. To solve the first stage optimization problem (29) and obtain the initial values for the second stage optimization, we prefer Gurobi [36], [37] which is appropriate to the changes of network demands. The computational complexity of solving the second stage optimization problem (30) increases rapidly as the number of FSO links, network size, and traffic demands grow. In this section, to avoid the computational complexity, we propose a suitable metaheuristic algorithm to gradually upgrade the bottleneck RF links with FSO links.

In [38] and [39], the authors have proved that ILS is a suitable and well performing algorithm for combinatorial optimization problems. The acceptance criteria, initial solution, and perturbation are the important components of ILS algorithm design [39]. Based on ILS, an IILSA is developed to obtain the high-quality solutions for our two-stage optimization in only a few seconds. In our IILSA, to find a pleasing starting point for local search, a heuristic method is adopted to rapidly obtain the initial solutions of IILSA. An appropriate perturbation is adopted to efficiently explore the solution space while keeping the search history in memory. Furthermore, at each iteration, some low-quality solutions which would not guide the search to the promising areas of search space are produced. In order to filter the low-quality solutions, a kind of simulated annealing schedule is used as the acceptance criterion. In Section V, we will investigate the performance of our IILSA and compare it with ILS and branch-and-cut algorithms.

We provide the pseudocode of our IILSA in Algorithm 1. Firstly, we use heuristic solution to find the initial value of x_{mn}^{i}. Lines 3 and 4 are used to perform constraint relaxations and obtain the initial value of x_{mn}^{i}. At each iteration, line 6 performs a perturbation of the local optimal solutions and obtains a new starting point for next local search. Based on the initial value of x_{mn}^{i}, the optimization problem (30) is solved in line 7. Lines 8-11 adopt annealing schedule to choose the acceptance criterion. $T = 0.025\ F[k]$ is a temperature parameter, $P_{th} \in [0,1]$ is a random number generated for each iteration, and $T_0 = 0.98$ is the decay factor [40]. Lines 13-22 assign the routing path from source s to destination d. Firstly, lines 15-18 traverse the logical links from s to d. Then, lines 19-21 choose the next-hop according to the maximum observation $Y_{mn,FSO}^{\omega}$. We judge intuitively that it implies the packets from ω are forwarded on the FSO logical link l_{mn}^{FSO} if the relaxed $Y_{mn,FSO}^{\omega}$ approaches 1. Otherwise, the packets from ω are not forwarded on l_{mn}^{FSO} if $Y_{mn,FSO}^{\omega}$ is close to 0. Similarly, lines 23-32 are used to obtain the values of the indicator variable $Y_{mn,i}^{\omega}$. We expect the packets from ω to be forwarded on

Algorithm 1 IILSA

1: **set** $D_{mn}^{FSO} = 1$, where{m, n} $= \min_{m,n,i,x_{mn}^i=1} \left(c_{mn}^i - \sum_{\omega} \lambda_{mn,i}^{\omega} \right)$.
2: **set** $K =$ the maximum number of iterations.
3: **solve** optimization problem (30) **subject to**
$0 \le x_{mn}^i \le 1, \forall m, n \in N, l_{mn} \in L, \forall i \in \{1, \cdots, C\}$,
$0 \le Y_{mn,FSO}^{\omega} \le 1, 0 \le Y_{mn,i}^{\omega} \le 1, \forall m, n \in N, l_{mn} \in L, \forall \omega \in S_D, \forall i \in \{1, \cdots, C\}$.
4: **set** $x_{mn}^i[1] = 1$ **where** {m, n, i} = argmax x_{mn}^i.
set $x_{mn}^i[1] = 0$ **where** {m, n, i}$\neq$ argmax x_{mn}^i.
5: **for** $k = 1$ **to** K **do**
6: $\{x_{mn}^i, p, q\} = perturbation(x_{mn}^i), F[0] = 0$.
7: **solve** the optimization problem (30) by using x_{mn}^i obtained in line 4,
subject to
$0 \le Y_{mn,FSO}^{\omega} \le 1, \ 0 \le Y_{mn,i}^{\omega} \le 1, \ \forall m, n \in N, l_{mn} \in L, \forall \omega \in S_D, \forall i \in \{1, \cdots, C\}$,
$x_{mn}^i = x_{mn}^i[k], \forall m, n \in N, l_{mn} \in L, m, n \notin \{p, q\}$.
8: **if** $F[k-1] < F[k]$, **then set**
$x_{mn}^i[k+1] = x_{mn}^i, \forall m, n \in N, l_{mn} \in L, \forall i \in \{1, \cdots, C\}$.
9: **else if** $\exp\left(-\frac{F[k]-F[k-1]}{T}\right) > P_{th}$, **then set**
$x_{mn}^i[k+1] = x_{mn}^i, \forall m, n \in N, l_{mn} \in L, \forall i \in \{1, \cdots, C\}$.
10: **end if**
11: **set** $T = T \cdot T_0$.
12: **end**
13: **for** each source and destination pair (s, d) **do**
14: **set** $m = s$.
15: **while** $m \neq d$ **do**
16: **set** $Y_{mn,FSO}^{\omega} = 1$, **where** $n = argmax_n Y_{mn,FSO}^{\omega}$.
17: **set** $m = n$.
18: **end**
19: **for** all $m, n \in N$ **do**
20: **if** $Y_{mn,FSO}^{\omega} \neq 1$, **then set** $Y_{mn,FSO}^{\omega} = 0$.
21: **end**
22: **end**
23: **for** each source and destination pair (s, d) **do**
24: **set** $m = s$.
25: **while** $m \neq d$ **do**
26: **set** $Y_{mn,i}^{\omega} = 1$, **where** $\{i, n\} = argmax_{i,n} Y_{mn,i}^{\omega}$.
27: **set** $m = n$.
28: **end**
29: **for** all $m, n \in N$ and all channels $i \in \{1, \ldots, C\}$ **do**
30: **if** $Y_{mn,i}^{\omega} \neq 1$, **then set** $Y_{mn,i}^{\omega} = 0$.
31: **end**
32: **end**

the logical link l_{mn}^{RF} over the i^{th} RF channel if the relaxed $Y_{mn,i}^{\omega}$ approaches 1. The computational complexity of the proposed IILSA is $\max(O(K), O(C|\omega||N|^2))$, which is polynomial in time.

Algorithm 2 Perturbation

1: **Input**: x_{mn}^i.
2: Randomly choose $p, q \in N$, such that $l_{pq} \in L$.
3: $Z_{RAN} = rand(0, 0.2)$, $Z_{fin} = floor(Z_{RAN}|L|)$.
4: **for** $Z^* = 1$ **to** Z_{fin} **do**
5: Randomly choose $m', n' \in N$, such that $l_{m'n'} \in L$.
6: **if** $\sum_i x_{mn}^i \geq 1$
7: Randomly choose one $i \in \{1, \ldots, C\}$, set $x_{mn}^i = 1$.
8: **end**
9: **end**

TABLE 2. Parameters.

Parameter	Symbol	Value
RF data rate	c^{RF}	100 Mbps
RF SNR threshold	ϕ	20 dB
RF noise power spectral density	N_0	-100 dBm
Reference distance	d_0	10 m
Path loss exponent	η	4
Transmit power	P_m	20 dBm
Nakagami parameter	U_k	1
Activity probability	χ_k	0.5
Chip factor	a	1
Shadowing factor	ζ_k	0
Spreading factor	W	1
FSO capacity	c^{FSO}	1 Gbps
FSO SNR threshold	γ_{th}	16 dB
FSO noise variance	$\sigma_{n_0}^2$	10^{-14} W
Receiver aperture diameter	r	20 cm
Responsivity	R	0.5 A/W
Wavelength	λ_1	1550 nm
Beam divergence angle	θ	2 mrad

The pseudocode of perturbation is provided in Algorithm 2. We use the perturbation to avoid being trapped in local optimum. Firstly, in every iteration, line 2 randomly selects a link l_{pq} with the goal of removing it from the solution space. Line 3 randomly selects a certain number of links. Then, some new solutions are added to enlarge the search space. Lines 4-9 generate new solutions to perturb the current optimal solutions, that is, randomly adding an RF channel between the node pair of a selected link. The perturbation is suitable for our problem, it is not too weak to make IILSA escape from local optimum, or too strong to make IILSA different from the random restart local search.

V. SIMULATION RESULTS AND DISCUSSIONS

To evaluate the performance of the proposed hybrid RF/FSO MCMR WMN architecture, simulation results are given based on the proposed two-stage optimization, Gurobi, and IILSA in this section. In our simulations, the values of weather-dependent variables and relevant parameters taken from [18], [25], and [31] are listed in Table 2 and Table 3, respectively.

A. OPTIMIZED CHANNEL ALLOCATION, INTERFACE ASSIGNMENT, AND LOGICAL TOPOLOGY

The impacts of the number of RF channels C and the number of RF NICs I are quantified in this subsection, and the optimized channel allocation, interface assignment, and logical

TABLE 3. Weather-dependent variables.

Weather Condition	$C_n^2 \times 10^{-14}[m^{-2/3}]$	α[dB/km]
Clear air	5.0	0.43
Moderate fog	0.2	35.38
Moderate rain	0.5	5.84

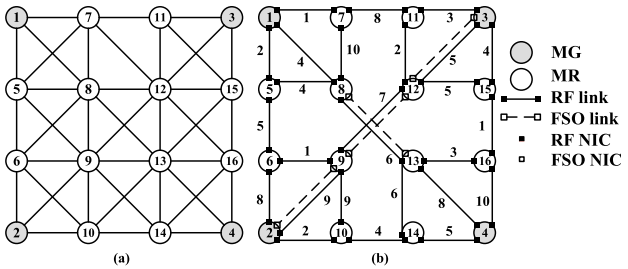

FIGURE 2. A 16-node grid network, (a) physical topology, (b) resulting FSO link allocation, channel allocation, interface assignment, and logical topology for our RA scheme.

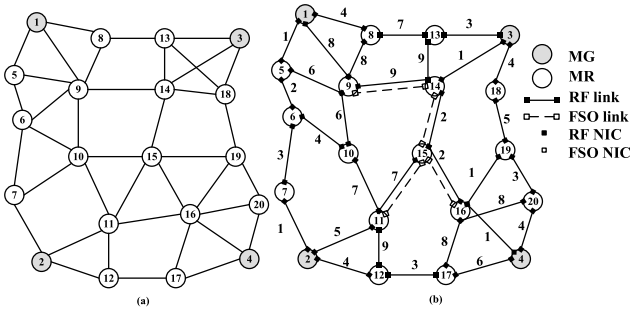

FIGURE 3. An example of 20-node randomly generated network, (a) physical topology, (b) resulting FSO link allocation, channel allocation, interface assignment, and logical topology for our RA scheme.

topology are also illustrated. We consider a sample physical topology of rectangular 4 × 4 nodes grid network shown in Fig. 2(a), whose vertical and horizontal neighboring nodes are in 2 km away from each other. To evaluate the full performance, we also consider a more ordinary 20 nodes randomly generated asymmetric physical topology, one of which is illustrated in Fig. 3(a). We assume that there are 4 nodes located at the vertices of a 10 km × 10 km square area, and the other nodes lie randomly in this square. In the above two network topologies, we assume that the nodes placed at the four corners serve as MGs, and there are four traffic demands (nodes 1 to 4, nodes 4 to 1, nodes 2 to 3, and nodes 3 to 2) diagonally across the network. Figure 4 plots the maximum network throughput of the physical topologies illustrated in Fig. 2(a) and Fig. 3(a) versus C, for various I and $M = 4$. As shown in Fig.4, when $I = 1$, the maximum throughput cannot be improved for increasing C. When $I = 2$ and $I = 3$, with the increase in C, the maximum throughput increases first and then stays stable. Similarly, given a fixed C, the maximum throughput increases with I. While there is an I for which the maximum throughput cannot be improved by installing more RF NICs. For example, in 16-node grid network, when $C = 5$, the maximum throughput is not improved by increasing I from 2 to 3.

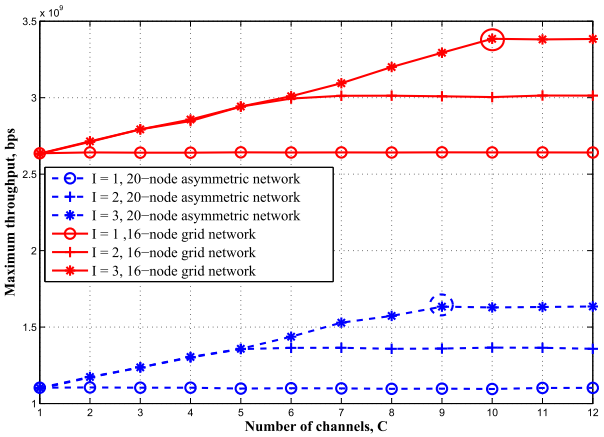

FIGURE 4. Maximum throughput versus number of channels.

The above observations indicate that the maximum throughput depends on the numbers of available RF channels and NICs, and sometimes it may not be improved by increasing only one of the numbers.

To illustrate our RA scheme, Fig. 2(b) and Fig. 3(b) show the corresponding logical topology, channel allocation, FSO link allocation, and interface assignment for Fig. 2(a) and Fig. 3(a), respectively. In Fig. 2(b) and Fig. 3(b), we consider the noted points in Fig.4 where $I = 3, C = 10$ and $I = 3, C = 9$, respectively. As Fig. 2(b) and Fig. 3(b) shown, the bottleneck RF logical links, that is, the congested RF logical links, are upgraded with FSO logical links. They also show that the available FSO links, RF channels, and NICs are fully utilized. These results indicate that our model formulation determines a reasonable RA scheme. It is also noteworthy that our model formulation tends to divide the overall network into subgraphs consisting of links which can be active simultaneously, and the FSO links are always allocated on the edges of the subgraphs.

B. IMPACT OF WEATHER CONDITION

Numerical results show the maximum throughput for various numbers of FSO links M under various weather conditions. We consider the grid topology with 16 MRs and asymmetric topology with 20 MRs illustrated in Fig. 2(a) and Fig. 3(a) respectively, and the traffic demands are also the same. We assume that $I = 3, C = 10$ and $I = 3, C = 9$, respectively. In Fig. 5(a), we show the maximum throughput under various weather conditions. As it is expected, the maximum throughput increases with M nearly linearly. It also can be seen that the weather conditions have a big impact upon the maximum throughput. The reason is that the FSO link availability π_{mn}^{FSO} depends strongly on the weather conditions, and π_{mn}^{FSO} affects the available link capacity and the capacity constraint given by Eq. (25).

We also consider a randomly generated larger-scale network with 60 nodes to evaluate the full performance of our IILSA. We assume that the 12 nodes located at the edges and vertices of a 15 km × 15 km square area serve as MGs, and the other nodes lie randomly in this square. The traffic demands are assumed to be between the source-destination

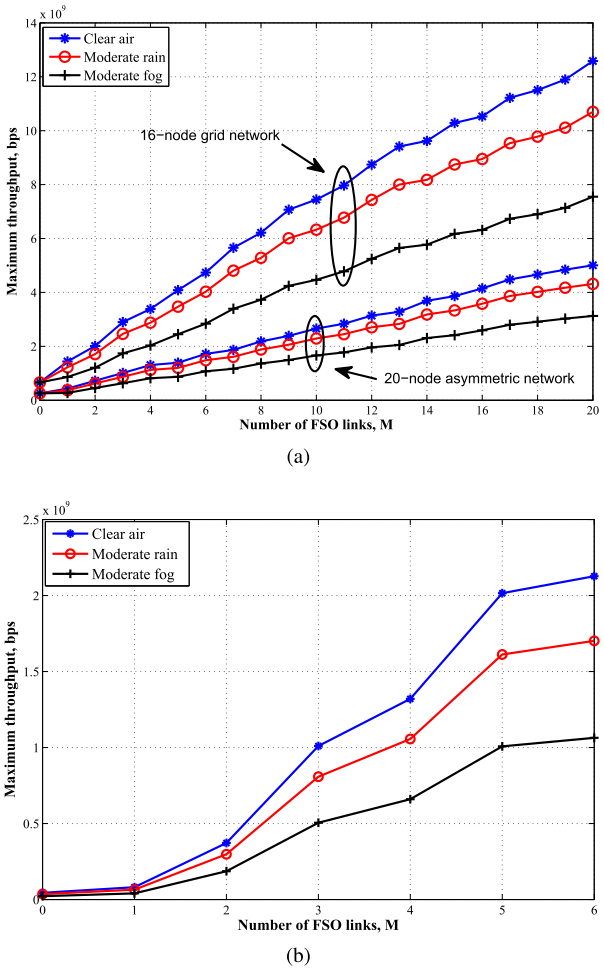

FIGURE 5. Maximum throughput versus number of FSO links under various weather conditions, (a) 16-node grid and 20-node asymmetric networks, (b) randomly generated network topology with 60 nodes.

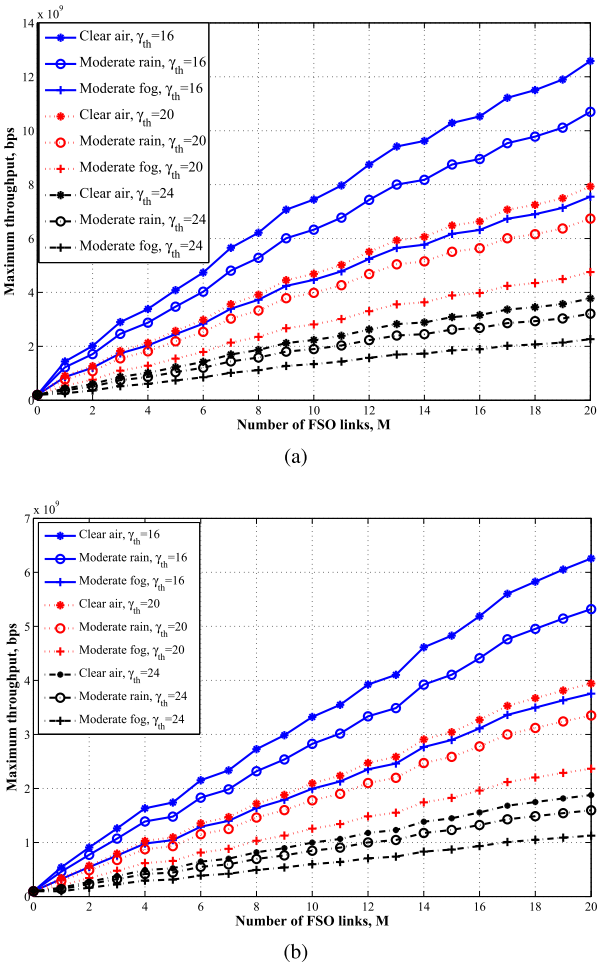

FIGURE 6. Maximum throughput versus number of FSO links under various weather conditions and different values of γ_{th}, (a) 16-node grid, (b) 20-node asymmetric network.

pairs consisting of these 12 MGs. We consider that $I = 3$ and $C = 9$. In Fig. 5(b), the maximum throughput versus M under various weather conditions for the above network is illustrated. As shown in Fig. 5(b), the proposed IILSA makes our two-stage optimization available for larger-scale networks. This is because the computational complexity of the proposed IILSA is polynomial in time. Furthermore, deserved to be mentioned, Fig. 5 verifies that it is worthy to augment MCMR WMN with FSO technologies, even though the availability of FSO links is not 100% under some weather conditions.

C. IMPACT OF FSO SNR THRESHOLD

Figure 6 illustrates the maximum throughput versus M under various weather conditions for the different values of FSO SNR threshold γ_{th}. In Fig. 6(a) and Fig. 6(b), we consider the same 16-node grid network and 20-node asymmetric topology illustrated in Fig. 2(a) and Fig. 3(a), respectively. And the traffic demands are also the same. We assume that $I = 3, C = 10$ and $I = 3, C = 9$, respectively. As we can see in Fig. 6, the trends of the 16-node grid network and more general 20-node asymmetric topology are similar, and γ_{th} has an effect on the maximum throughput. This is because that π_{mn}^{FSO} decreases as γ_{th} increases.

D. IMPACT OF DELAY

Considering the topology illustrated in Fig. 2(a) and Fig. 3(a) and the same traffic demands, the impact of delay is investigated by varying the tunable parameter ξ. We consider that $I = 3, C = 10$ and $I = 3, C = 9$, respectively. Figure 7 plots the maximum throughput versus ξ. As can be seen in Fig. 7, the general trends of the regular 16-node grid topology and random 20-node asymmetric topology are similar. The maximum throughput is minimal when $\xi = 1$ and improves slightly as ξ increases. However, the trend of throughput improvement slows down as ξ increases. There is an evident tradeoff between the network throughput and delay requirement. The network resource cannot be utilized efficiently under the tight delay constraint (i.e., $\xi = 1$), whereas the solution space may be enlarged as the delay constraint is relaxed, which may increase the network throughput.

E. PERFORMANCE COMPARISON OF IILSA, ILS ALGORITHM, AND BRANCH-AND-CUT ALGORITHM

In the following, we show the performance of the proposed IILSA, and compare it with ILS [20], [41] and branch-and-cut algorithms [42]. Considering the 16-node grid

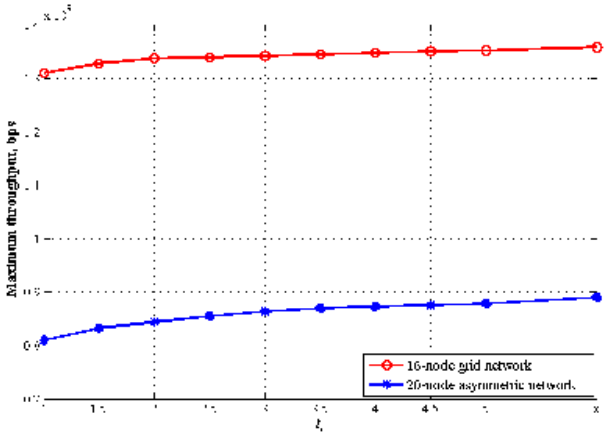

FIGURE 7. Maximum throughput versus ξ.

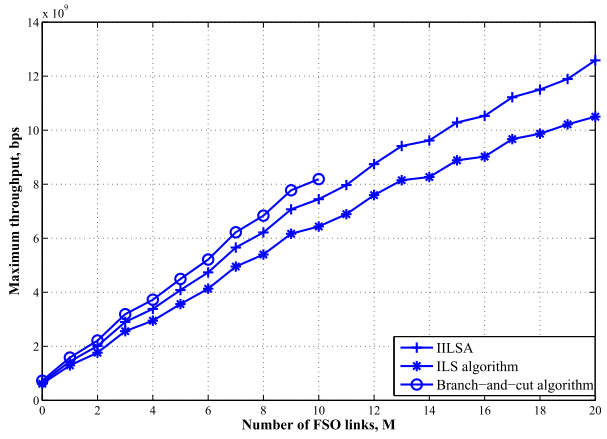

(a)

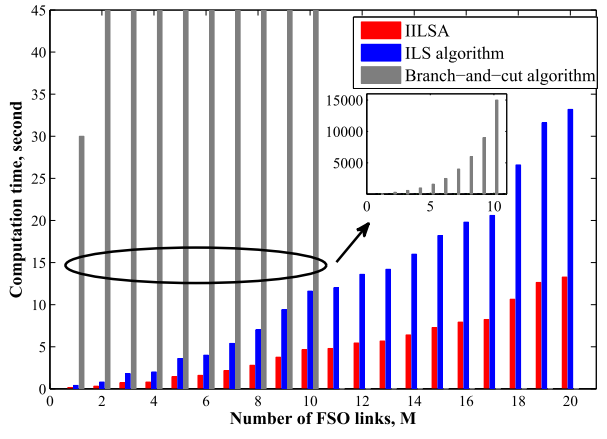

(b)

FIGURE 8. Comparisons of IILSA, ILS algorithm, and branch-and-cut algorithm for different numbers of FSO links, (a) maximum throughput, (b) computation time.

network shown in Fig. 2(a) and the same traffic demands, Fig. 8 illustrates the maximum throughput and computation time for IILSA, ILS algorithm, and branch-and-cut algorithm. We assume that $I = 3$ and $C = 10$. As can be seen in Fig. 8(a), the throughput enhancement trends of IILSA, branch-and-cut algorithm, and ILS algorithm are similar.

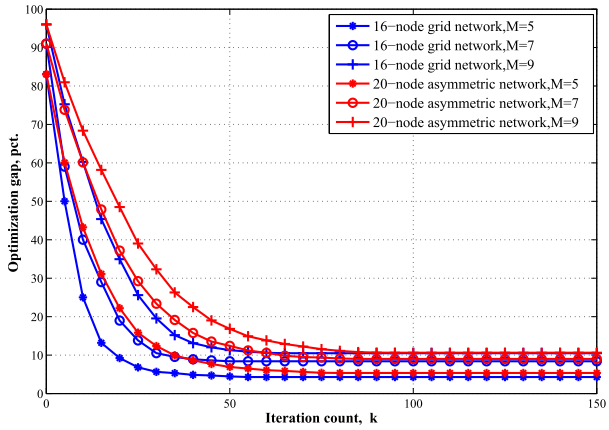

FIGURE 9. Optimization gap versus iteration count for different values of M.

We only show results of the branch-and-cut algorithm which obtains the exact optimal solutions for $M \leq 10$, because its computational complexity is exponential in time and its runtime becomes excessive for a larger value of M. By contrast, the proposed IILSA makes our optimization problem solvable in polynomial time in practice. It indicates that in terms of the maximum throughput, the proposed IILSA is slightly inferior to the branch-and-cut algorithm, while in terms of the computational complexity, the branch-and-cut algorithm is considerably larger than our IILSA. From Fig. 8(a), we also clearly see that our IILSA obtains the better near-optimal solutions compared with the ILS algorithm. In Fig. 8(b), we compare the runtime of our IILSA with that of ILS and branch-and-cut algorithms. It is obvious that our IILSA spends less time than ILS and branch-and-cut algorithms, which is important in practice.

To investigate the convergent performance of IILSA, we measure the gap between the exact solution F_{exa} and the solution $F[k]$ obtained by IILSA for the k^{th} iteration. The exact optimal solutions are obtained from branch-and-cut algorithm. We consider the above mentioned 16-node grid network and 20-node asymmetric topology, and the traffic demands, RF NICs, and available channels are also the same. The gap is defined as $(F_{exa} - F[k])/F_{exa}$. In Fig. 9, we illustrate the relationship between the gap and iteration count k for different values of M. As can be seen, for the 16-node grid network, the gap decreases sharply with the increase of k when about $k < 60$. And the gap gradually tends to 0 after about $k \geq 60$. This observation shows that the proposed IILSA can converge within a limited iteration count. In our simulation, we choose an appropriate maximum iteration number K according to the convergent property (e.g., $K = 60$ and $K = 80$ for the 16-node grid and 20-node asymmetric networks, respectively).

VI. CONCLUSION

In this paper, we introduced a throughput improvement method for MCMR WMN and constructed a hybrid RF/FSO MCMR WMN topology. In this hybrid network, we jointly formulated the RA problem as a two-stage optimization

problem which incorporates the FSO link availability under various weather conditions and the fading nature of RF links. Our two-stage optimization model was formulated as an MILP in each stage so as to maximize the network throughput, while fairness to all given traffic demands was guaranteed and the delay requirement was satisfied. To reduce the computational complexity, we proposed a low-complexity IILSA to solve our two-stage optimization problem. We obtained the relationships between the network throughput and the delay requirement, FSO SNR threshold, weather conditions, available RF channels and NICs, and number of FSO links, respectively. The relationships provide insights for network planning. Simulation results show that our model formulation determines reasonable RA and our IILSA can obtain high-quality solutions for our optimization problem in an acceptable runtime. They also reveal that the network throughput can be improved dramatically by upgrading the bottleneck RF links with FSO links and augmenting MCMR WMN with FSO technologies is worthwhile. In the future, we desire to take the mobility into account and extend our work to the hybrid RF/FSO VANET.

REFERENCES

[1] H. Wang, K.-W. Chin, and S. Soh, "On minimizing data forwarding schedule in multi transmit/receive wireless mesh networks," *IEEE Access*, vol. 4, pp. 1570–1582, 2016.

[2] M. Malnar, N. Neskovic, and A. Neskovic, "A new quality of service aware multi-channel multi-interface link layer protocol for wireless mesh networks," *Wireless Netw.*, vol. 21, no. 3, pp. 727–738, Apr. 2015.

[3] Y. Wu, F. Hu, S. Kumar, J. D. Matyjas, Q. Sun, and Y. Zhu, "Apprenticeship learning based spectrum decision in multi-channel wireless mesh networks with multi-beam antennas," *IEEE Trans. Mobile Comput.*, vol. 16, no. 2, pp. 314–325, Feb. 2017.

[4] Y. Qu, B. Ng, and W. Seah, "A survey of routing and channel assignment in multi-channel multi-radio WMNs," *J. Netw. Comput. Appl.*, vol. 65, pp. 120–130, Apr. 2016.

[5] B. Makki, T. Svensson, M. Brandt-Pearce, and M.-S. Alouini, "Performance analysis of RF-FSO multi-hop networks," in *Proc. IEEE Wireless Commun. Netw. Conf. (WCNC)*, Mar. 2017.

[6] F. Ahdi and S. Subramaniam, "Capacity enhancement of RF wireless mesh networks through FSO links," *J. Opt. Commun. Netw.*, vol. 8, no. 7, pp. 495–506, Jul. 2016.

[7] M. Najafi, V. Jamali, and R. Schober, "Optimal relay selection for the parallel hybrid RF/FSO relay channel: Non-buffer-aided and buffer-aided designs," *IEEE Trans. Commun.*, vol. 65, no. 7, pp. 2794–2810, Jul. 2017.

[8] V. Jamali, D. S. Michalopoulos, M. Uysal, and R. Schober, "Link allocation for multiuser systems with hybrid RF/FSO backhaul: Delay-limited and delay-tolerant designs," *IEEE Trans. Wireless Commun.*, vol. 15, no. 5, pp. 3281–3295, May 2016.

[9] M. Lu, L. Liu, and S. Hranilovic, "Raptor-coded free-space optical communications experiment," *J. Opt. Commun. Netw.*, vol. 8, no. 6, pp. 398–407, Jun. 2016.

[10] M. Khan, S. Bhunia, M. Yuksel, and S. Sengupta, "LOS discovery in 3D for highly directional transceivers," in *Proc. IEEE Mil. Commun. Conf. (MILCOM)*, Dec. 2016, pp. 325–330.

[11] M. Khan, S. Bhunia, M. Yuksel, and L. C. Kane, "Line-of-sight discovery in 3D using highly directional transceivers," *IEEE Trans. Mobile Comput.*, vol. 18, no. 12, pp. 2885–2898, Dec. 2019.

[12] F. Ahdi and S. Subramaniam, "Improving hybrid FSO/RF network reliability through transceiver reconfiguration," in *Proc. IEEE Global Commun. Conf. (GLOBECOM)*, Dec. 2012, pp. 2947–2952.

[13] O. Awwad, A. Al-Fuqaha, B. Khan, and G. B. Brahim, "Topology control schema for better QoS in hybrid RF/FSO mesh networks," *IEEE Trans. Commun.*, vol. 60, no. 5, pp. 1398–1406, May 2012.

[14] A. Douik, H. Dahrouj, T. Y. Al-Naffouri, and M.-S. Alouini, "Hybrid radio/free-space optical design for next generation backhaul systems," *IEEE Trans. Commun.*, vol. 64, no. 6, pp. 2563–2577, Jun. 2016.

[15] Y. Zhao, W. Shi, H. Shi, W. Liu, and P. Wu, "Joint transmission slot assignment, FSO links allocation and power control for hybrid RF/FSO wireless mesh networks," *Current Opt. Photon.*, vol. 1, no. 4, pp. 325–335, Aug. 2017.

[16] K. Zhou, C. Gong, N. Wu, and Z. Xu, "Distributed channel allocation and rate control for hybrid FSO/RF vehicular ad hoc networks," *J. Opt. Commun. Netw.*, vol. 9, no. 8, pp. 669–681, Aug. 2017.

[17] Y. Wu, Q. Yang, D. Park, and K. S. Kwak, "Dynamic link selection and power allocation with reliability guarantees for hybrid FSO/RF systems," *IEEE Access*, vol. 5, pp. 13654–13664, 2017.

[18] Y. Tang and M. Brandt-Pearce, "Link allocation, routing, and scheduling for hybrid FSO/RF wireless mesh networks," *J. Opt. Commun. Netw.*, vol. 6, no. 1, pp. 86–95, Jan. 2014.

[19] I. W.-H. Ho, P. P. Lam, P. H. J. Chong, and S. C. Liew, "Harnessing the high bandwidth of multiradio multichannel 802.11n mesh networks," *IEEE Trans. Mobile Comput.*, vol. 13, no. 2, pp. 448–456, Feb. 2014.

[20] A. Mohsenian-rad and V. S. Wong, "Joint logical topology design, interface assignment, channel allocation, and routing for multi-channel wireless mesh networks," *IEEE Trans. Wireless Commun.*, vol. 6, no. 12, pp. 4432–4440, Dec. 2007.

[21] F. Martignon, S. Paris, I. Filippini, L. Chen, and A. Capone, "Efficient and truthful bandwidth allocation in wireless mesh community networks," *IEEE/ACM Trans. Netw.*, vol. 23, no. 1, pp. 161–174, Feb. 2015.

[22] A. A. Almohammedi, N. K. Noordin, A. Sali, F. Hashim, and M. Balfaqih, "An adaptive multi-channel assignment and coordination scheme for IEEE 802.11P/1609.4 in vehicular ad-hoc networks," *IEEE Access*, vol. 6, pp. 2781–2802, 2018.

[23] J. Luo, C. Rosenberg, and A. Girard, "Engineering wireless mesh networks: Joint scheduling, routing, power control, and rate adaptation," *IEEE/ACM Trans. Netw.*, vol. 18, no. 5, pp. 1387–1400, Oct. 2010.

[24] Y. Chen and C. W. Sung, "Characterization of SINR region for multiple interfering multicast in power-controlled systems," *IEEE Trans. Commun.*, vol. 67, no. 1, pp. 165–175, Jan. 2019.

[25] D. Torrieri and M. C. Valenti, "The outage probability of a finite ad hoc network in Nakagami fading," *IEEE Trans. Commun.*, vol. 60, no. 11, pp. 3509–3518, Nov. 2012.

[26] M. A. Esmail, H. Fathallah, and M.-S. Alouini, "On the performance of optical wireless links over random foggy channels," *IEEE Access*, vol. 5, pp. 2894–2903, 2017.

[27] H. Singh and A. S. Sappal, "Moment-based approach for statistical and simulative analysis of turbulent atmospheric channels in FSO communication," *IEEE Access*, vol. 7, pp. 11296–11317, 2019.

[28] M. Smadi, S. Ghosh, A. Farid, T. Todd, and S. Hranilovic, "Free-space optical gateway placement in hybrid wireless mesh networks," *J. Lightw. Technol.*, vol. 27, no. 14, pp. 2688–2697, Jul. 15, 2009.

[29] M. T. Dabiri and S. M. S. Sadough, "Performance analysis of all-optical amplify and forward relaying over log-normal FSO channels," *J. Opt. Commun. Netw.*, vol. 10, no. 2, pp. 79–89, Feb. 2018.

[30] H. Alquwaiee, H.-C. Yang, and M.-S. Alouini, "On the asymptotic capacity of dual-aperture FSO systems with generalized pointing error model," *IEEE Trans. Wireless Commun.*, vol. 15, no. 9, pp. 6502–6512, Sep. 2016.

[31] H. Kazemi, M. Uysal, F. Touati, and H. Haas, "Outage performance of multi-hop hybrid FSO/RF communication systems," in *Proc. 4th Int. Workshop Opt. Wireless Commun. (IWOW)*, Sep. 2015, pp. 83–87.

[32] F. Nadeem, V. Kvicera, M. Awan, E. Leitgeb, S. Muhammad, and G. Kandus, "Weather effects on hybrid FSO/RF communication link," *IEEE J. Sel. Areas Commun.*, vol. 27, no. 9, pp. 1687–1697, Dec. 2009.

[33] A. K. Majumdar, "Free-space laser communication performance in the atmospheric channel," *J. Opt. Fiber Commun. Rep.*, vol. 2, no. 4, pp. 345–396, Oct. 2005.

[34] I. Son, S. Mao, and S. K. Das, "On the design and optimization of a free space optical access network," *Opt. Switching Netw.*, vol. 11, pp. 29–43, Jan. 2014.

[35] M. A. Khalighi and M. Uysal, "Survey on free space optical communication: A communication theory perspective," *IEEE Commun. Surveys Tuts.*, vol. 16, no. 4, pp. 2231–2258, Jun. 2014.

[36] *Gurobi Optimization*. Accessed: Oct. 27, 2018. [Online]. Available: http://www.gurobi.com/

[37] J. Yang, J. Zhao, F. Wen, and Z. Y. Dong, "A framework of customizing electricity retail prices," *IEEE Trans. Power Syst.*, vol. 33, no. 3, pp. 2415–2428, May 2018.

[38] P. Vansteenwegen, W. Souffriau, G. V. Berghe, and D. Van Oudheusden, "Iterated local search for the team orienteering problem with time windows," *Comput. Oper. Res.*, vol. 36, no. 12, pp. 3281–3290, Dec. 2009.
[39] L. Jiang, H. Chang, S. Zhao, J. Dong, and W. Lu, "A travelling salesman problem with carbon emission reduction in the last mile delivery," *IEEE Access*, vol. 7, pp. 61620–61627, 2019.
[40] M. A. Cruz-Chavez, M. H. C. Rosales, J. C. Zavala-Diaz, J. A. H. Aguilar, A. Rodriguez-Leon, J. C. P. Avelino, M. E. L. Ortiz, and O. H. Salinas, "Hybrid micro genetic multi-population algorithm with collective communication for the job shop scheduling problem," *IEEE Access*, vol. 7, pp. 82358–82376, 2019.
[41] E. A. Lemamou, P. Galinier, and S. Chamberland, "A hybrid iterated local search algorithm for the global planning problem of survivable 4G wireless networks," *IEEE/ACM Trans. Netw.*, vol. 24, no. 1, pp. 137–148, Feb. 2016.
[42] A. Lucena and J. E. Beasley, "Branch and cut algorithms," in *Advances in Linear and Integer Programming*, J. E. Beasley, Ed. Oxford, U.K.: Oxford Univ. Press, 1996.

YAN ZHAO received the B.Eng. degree from the School of Information and Communication Engineering, North University of China, Taiyuan, China, in 2010, and the M.S. degree from the College of Information Engineering, Taiyuan University of Technology, Taiyuan, in 2014. She is currently pursuing the Ph.D. degree with the Department of Communications Engineering, Jilin University, Changchun, China. Her research interests include capacity planning of hybrid optical and wireless networks, resource allocation schemes, optimization, free space optical communication systems and networks, and wireless mesh networks.

WENXIAO SHI received the B.Eng. degree in communications engineering from the Changchun Institute of Posts and Telecommunications, Changchun, China, in 1983, the M.S. degree in electrical engineering from the Harbin Institute of Technology, Harbin, China, in 1991, and the Ph.D. degree in communication and information systems from Jilin University, Changchun, in 2006.

He is currently a Professor with the Department of Communications Engineering, Jilin University. His research interests include resource management, access control and load balance of heterogeneous wireless networks, wireless mesh networks, free space optical communications, and mobile edge computing.

HANYANG SHI received the B.Eng. degree from the School of Computer Science and Engineering, Changchun University of Technology, Changchun, China, in 2011, and the M.S. degree from the College of Information Engineering, Taiyuan University of Technology, Taiyuan, China, in 2014. He is currently pursuing the Ph.D. degree with the Department of Communications Engineering, Jilin University, Changchun. His research interests include free space optical communications, wireless communications theory, and indoor visible light communications.

WEI LIU received the B.Eng., M.S., and Ph.D. degrees from the Department of Communications Engineering, Jilin University, Changchun, China, in 2009, 2012, and 2015, respectively. She is currently an Assistant Professor with the Department of Communications Engineering, Jilin University. Her research interests include atmospheric channel compensation technology of free space optical communications, free space optical communications, and adaptive optics.

ZHUO WANG received the B.Eng. degree from the Department of Communications Engineering, Jilin University, Changchun, China, in 2017, where she is currently pursuing the Ph.D. degree. Her main research interest is the performance analysis of mixed radio frequency/free space optical relay systems.

JIADONG ZHANG received the B.Eng. degree from the Department of Communications Engineering, Jilin University, Changchun, China, in 2018, where he is currently pursuing the Ph.D. degree. His research interests include resource allocation for wireless networks, resource management in mobile edge computing, and computing offloading algorithm.